



International Conference on Case Histories in Geotechnical Engineering (1984) - First International Conference on Case Histories in Geotechnical Engineering

08 May 1984, 10:15 am - 5:00 pm

Deep Seated Base Failure and Reconstruction Work

M. Fukuoka

Science University of Tokyo, Noda City, Japan

Follow this and additional works at: <https://scholarsmine.mst.edu/icchge>



Part of the [Geotechnical Engineering Commons](#)

Recommended Citation

Fukuoka, M., "Deep Seated Base Failure and Reconstruction Work" (1984). *International Conference on Case Histories in Geotechnical Engineering*. 7.

<https://scholarsmine.mst.edu/icchge/1icchge/1icchge-theme3/7>

This Article - Conference proceedings is brought to you for free and open access by Scholars' Mine. It has been accepted for inclusion in International Conference on Case Histories in Geotechnical Engineering by an authorized administrator of Scholars' Mine. This work is protected by U. S. Copyright Law. Unauthorized use including reproduction for redistribution requires the permission of the copyright holder. For more information, please contact scholarsmine@mst.edu.

Deep Seated Base Failure and Reconstruction Work

M. Fukuoka

Professor of Civil Engineering, Science University of Tokyo, Noda City, Japan

SYNOPSIS As an embankment was constructed on thick soft clay ground, a deep seated failure took place. A large horizontal and vertical deformation was observed along the suspected sliding surface of the deep seated failure, when sand compaction piles were driven into the foundation for the purpose of soil improvement. After the soil improvement, an embankment was going to be reconstructed, but a sliding along the old sliding surface was feared. Since the amount of lateral movement was small, effectiveness of the sand compaction piles was ascertained. This paper presents a case record of this work.

INTRODUCTION

There are many different kinds of methods for improving deep soft ground under an embankment such as sand drain with deep wells, sand compaction piles, gravel piles, precast concrete piles, lime piles, and so on. Comparing these methods, it was found that the sand compaction pile was the most economical and reliable. Unexpected large horizontal and vertical displacement was observed along the old sliding surface. Therefore, another sliding was feared when an embankment load was applied on the improved ground. Stability analysis was made based on an assumption, and construction work followed with careful observations. Displacement was unexpectedly small and the embankment was constructed without fear of collapse. This paper presents the observed data and soil properties.

DEEP SEATED FAILURE OF EMBANKMENT FOUNDATION

Soil investigation for a soft foundation under embankment contains undisturbed sampling of clay and unconfined compression tests with these samples. Usually unconfined compressive strength q_u of the samples increase in direct proportion to the depth. Stability analysis is made using cohesion $c=q_u/2$ neglecting the angle of internal friction ϕ . As a circular sliding surface is applied, the depth of sliding may not be very deep. If the factor of safety is nearly equal to or a little less than 1, vertical drain method may be applied in order to accelerate settlement. Expecting the increase in soil strength, construction work may be done slowly. When the factor of safety is very low and budget is limited, the embankment may be constructed very slowly by lifting its height little by little. Sometimes stability analysis is made based on effective stress method using c' and ϕ' with pore pressure taking into account. The stability analysis of this example was made

along this line. The embankment was 4 m high and approximately 30 m wide. A circle giving the lowest factor of safety $F_s=1.27$ is shown in Fig. 1. Though it was thought that the embankment of this height could be constructed safely, careful construction work had been done with taking long construction period of 3 months. Sliding failure occurred without warning about 10 days after the completion of filling operation. Nothing happened that might trigger the sudden rupture except a small earthquake which took place a few days before the rupture. According to the result of survey, the ground surface changed in its shape as shown in Fig. 1. The center of the embankment sank down about 10 m, and many cracks appeared everywhere. Surprisingly, the crown of the embankment went down about 8 m below the original ground level. The south foot of the embankment moved almost 10 m outwards horizontally. The Block C was heaved about 5 m. The total length from top to tongue was about 150 m. According to the change of the ground, it was obvious that the rupture seemed not to be classified into an ordinary sliding surface. Soil investigation for clarifying the cause of rupture was carried out. A part of the result is shown in Fig. 1. There is a firm sand layer about 30 m deep under the soft layer. The compressive strength q_u is relatively large in proportion to the depth under the embankment, but it becomes smaller near the bottom sand layer. The ground from 80 m to 150 m on the horizontal scale is relatively uniform and unconfined compressive strengths are very low. Cone resistance with Dutch cone is also very low compared to that of the ground under the embankment. A composite sliding surface based on the investigation data is shown in Fig. 1 with a chain line. The sliding surface seems to pass the clay layer immediately above the firm sand layer, because a very sensitive clay was produced by leaching of salt which had been contained in clay layer deposited in sea. The characteristics of the clay is similar to the Scandinavian quick clay and sensitive. The

clay is apt to decrease its strength and begin to slide some excitation. The original ground surface inclined by 3.8 degrees, and shear force acted along the deep seated sliding surface even at ordinary time. The shear stress increased in the form of long lasted

movement velocity of this sliding soil mass. The following equation of motion with respect to the Block B.

$$m \frac{d^2 s}{dt^2} = \Delta P - c_u L \text{ -----(1)}$$

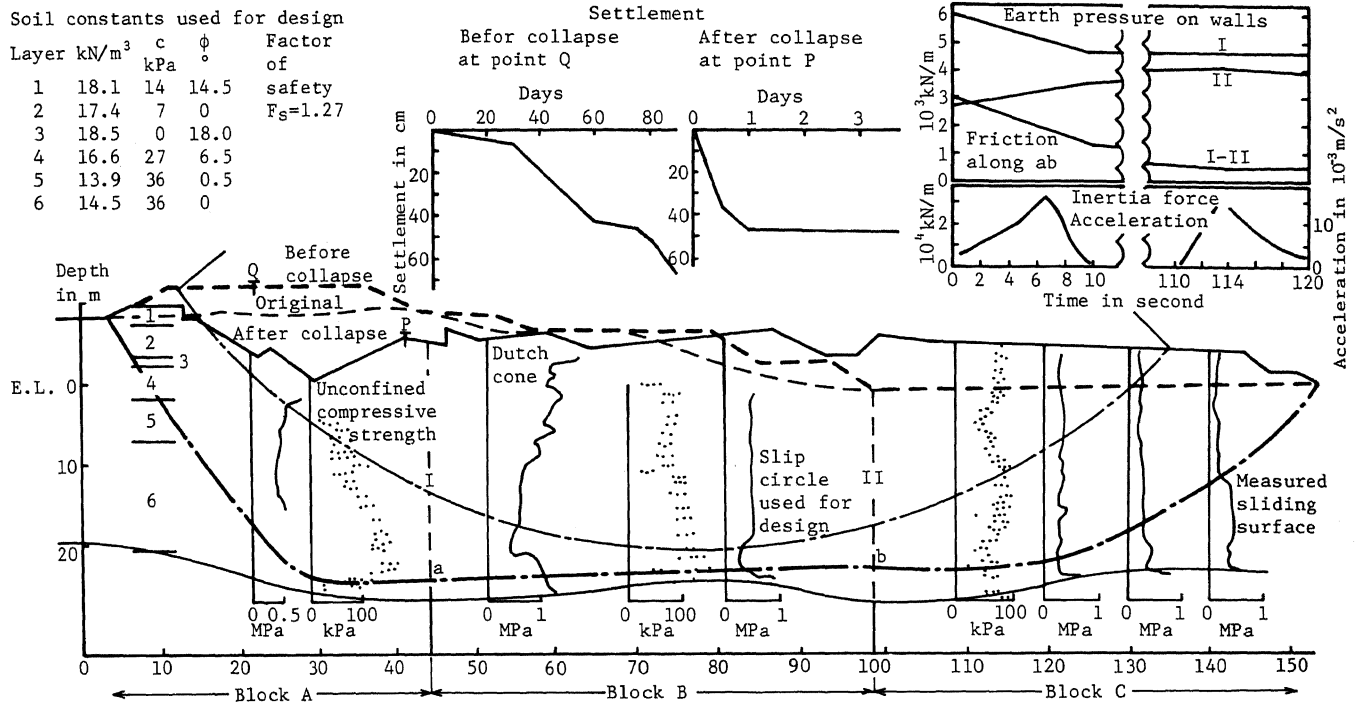


Fig. 1 Cross Section of Embankment

stress with embankment load. Sometimes sliding failure takes place after a certain period of time, when load is applied in the form of long lasted stress. The sliding failure occurred about 10 days after completion. Decrease of unconfined compressive strength was observed with clay samples from the ground under long lasted load as well. Mechanism of the sliding such as the change in soil strength and the speed of movement are estimated as follows. The sliding soil mass was divided into Blocks A, B, and C. The Blocks A, B, and C are active, transitional and passive part of the sliding soil mass, respectively. Planes I and II are the assumed vertical walls separating each block. Horizontal components of earth pressure against Walls I and II were about 6 and 3 MN/m, respectively, before the rupture. The total shear stress along the surface ab is 3 MN/m. The average shear stress was about 54 kPa, as the length of ab is about 56 m. As to shear stress distribution, shear stress near the Point a was larger than that near the Point b, because the former was influenced by the embankment load. The calculated shear stress is similar to the shear strength or cohesion $c = q_u/2$ obtained from the testing. Incipient failure took place and sliding surface began to form somewhere. But after the sliding surface is formed, shear resistance changes into dynamic from static one. Then the shear resistance decreases remarkably. The shear resistance may be calculated back from the

where

m: mass of Block B, s: distance, t: time,
 ΔP : pressure difference between Walls I and II
 $c_u L$: shear resistance along the surface ab.

Several workers were riding in a bus staying on the crown of the embankment. They reported that the sliding movement finished in about 2 minutes. The acceleration and inertia force were calculated by using the equation (1), and then the frictional force was obtained as shown in Fig. 1. The pressure difference, ΔP , change with time, mainly because of the sinking of Block A and the rising of Block B. As this calculation was made on the basis of a very bold assumption, the figures given in Fig. 1 might not be reliable. If we had measured movement of soil mass, more reliable analysis could have been made. This would be sufficient only to get a rough idea concerning mechanism of movement. The sliding movement was initiated by Block B, Block C was pushed away, and Block A followed. This mechanism would be proved by the fact that the Point P at the crown of the embankment in Fig. 1 continued to move for at least one day after the sliding. The kinetic friction along this surface ab is estimated at 0.5 MN/m, which is one sixth of the friction at the beginning of the sliding motion. As this example shows, stability problem in soil mechanics should be discussed not only for the viewpoint of the static failure but also of the dynamic behavior after complete sliding surface is formed and further the sliding soil mass is

travelling out of the sliding plane. Case records as this example would be a key to solve this sort of problems.

OUTLINE OF TOPOGRAPHY AND SOIL PROFILE

Figure 2 shows a plan of the site. The ground surface slopes from north to south, and its inclination is 1:16. E-W is the center of the embankment. Four meter high embankment slid towards south and made the scarp as shown in the figure. Sand compaction piles were going to be driven in the area shown in the figure in order to improve the soft ground. Along the N-S line, boring, Dutch cone and Swedish weight sounding test, pore water pressure measurement were conducted. Figure 1 shows a part of the test results; unconfined compression and Dutch cone tests. At the center of the embankment, the 10 m sandy clay layer near the ground surface showed relatively high cone resistance, but the clay layer very low. A firm sand layer was at the bottom. Unconfined compressive strength of the sandy clay layer was low, because it contained many sand seams. The unconfined compressive strength of the clay layer was 100-160 kPa. The boring point located outside the embankment gave the lower cone resistance and unconfined compressive strength. The unit weight of the sandy clay and clay were 16-18 and 14 kN/m³, respectively. The pore water pressure at the middle of the clay layer was 220 kPa which compares 120 kPa of the theoretical one.

INSTRUMENTATION

Prior to the sand compaction pile driving, uneven ground surface was levelled. One meter thick sand mat was laid on the ground surface. Figure 3 shows an arrangement of instrumentation. The inclinometer I-2, piezometers, total horizontal earth pressure cells were installed at the time after the construction of the sand mat and before the sand compaction pile (SCP) driving at the point marked I-2 in the figure. The total horizontal earth pressure cell has subjected to horizontal earth pressure. Two cells were installed at the two different depths from the beginning to avoid the time lag in measurement.

DRIVING OF SAND COMPACTION PILES (SCP)

A mandrel for SCP was a steel tube having the outer diameter of 0.5 m, and SCP had the diameter of 0.7 m after being compacted with a vibrator mounted at the top of the mandrel. The average length of the SCP was 31 m. The SCP were driven at each corner of a square mesh. The spacing of the SCP was 2 m. The maximum grain size of sands was 5 mm, and diameters of the sand grains were $D_{60}=1.0$ and $D_{10}=0.2$ mm. The pile driving work was conducted from July to November having intermission in August and September. The SCP driving started from the south row. Stage 1 was from July 8 to 28, Stage 2 from July 29 to October 12, Stage 3 from October 30 to November 8. Those stages are illustrated in Fig. 4.

GROUND MOVEMENT DURING SCP DRIVING

Ground movement during SCP driving was measured

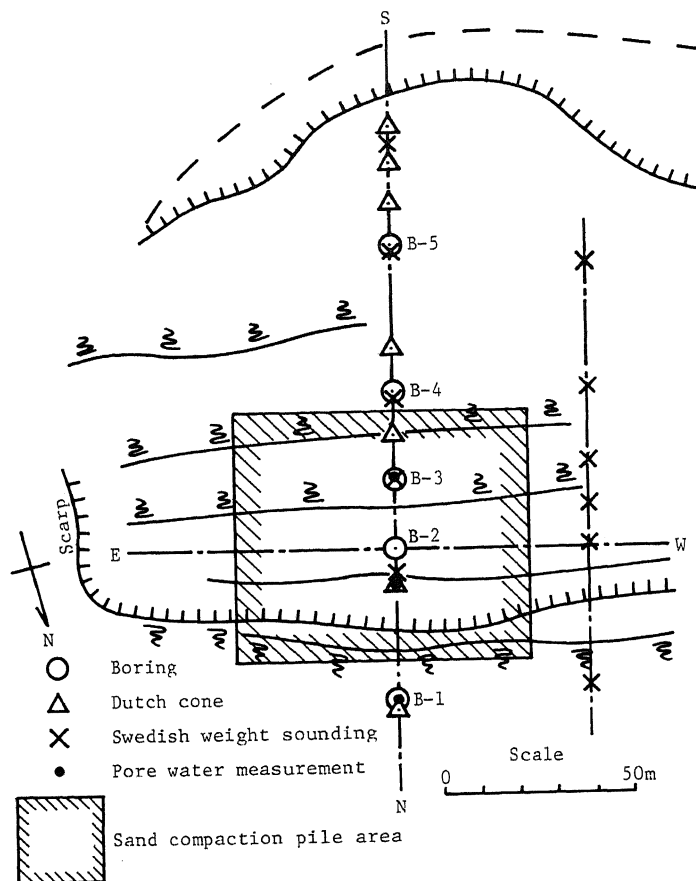


Fig. 2 Plan of the Test Site

with stakes driven on the ground surface, strain meters and inclinometers. Horizontal movement measured are shown in Fig. 4 (a) with contour lines. The maximum horizontal movement, as large as 130 m, was observed near the south foot of the sand mat marked as I-2. Figure 4 (b) shows vertical movement. The area which was located 20 to 40 m from the south foot of the sand mat showed large movement, and the largest one was 50 cm. Unexpected large movement was observed near the south edge of the sand mat. Judging from it, a kind of rotational sliding might have occurred at this part. Movement of the point marked 130 is given in Table I.

TABLE I. Movement of Ground at Point 130

Stage	Movement in cm	
	Horizontal	Vertical
1	50	15
2	50	20
3	30	15
Total	130	50

The area where the ground movement was observed was about 120 m south from the intersection of the lines NS and EW, and this exactly coincided with the previously slid area. At the point I-2, which was near the south foot of the sand mat, an inclinometer, pore water pressure meters and total horizontal pressure cells were installed. Figure 5 shows the order of the sand pile driving. Piles driven on July 9

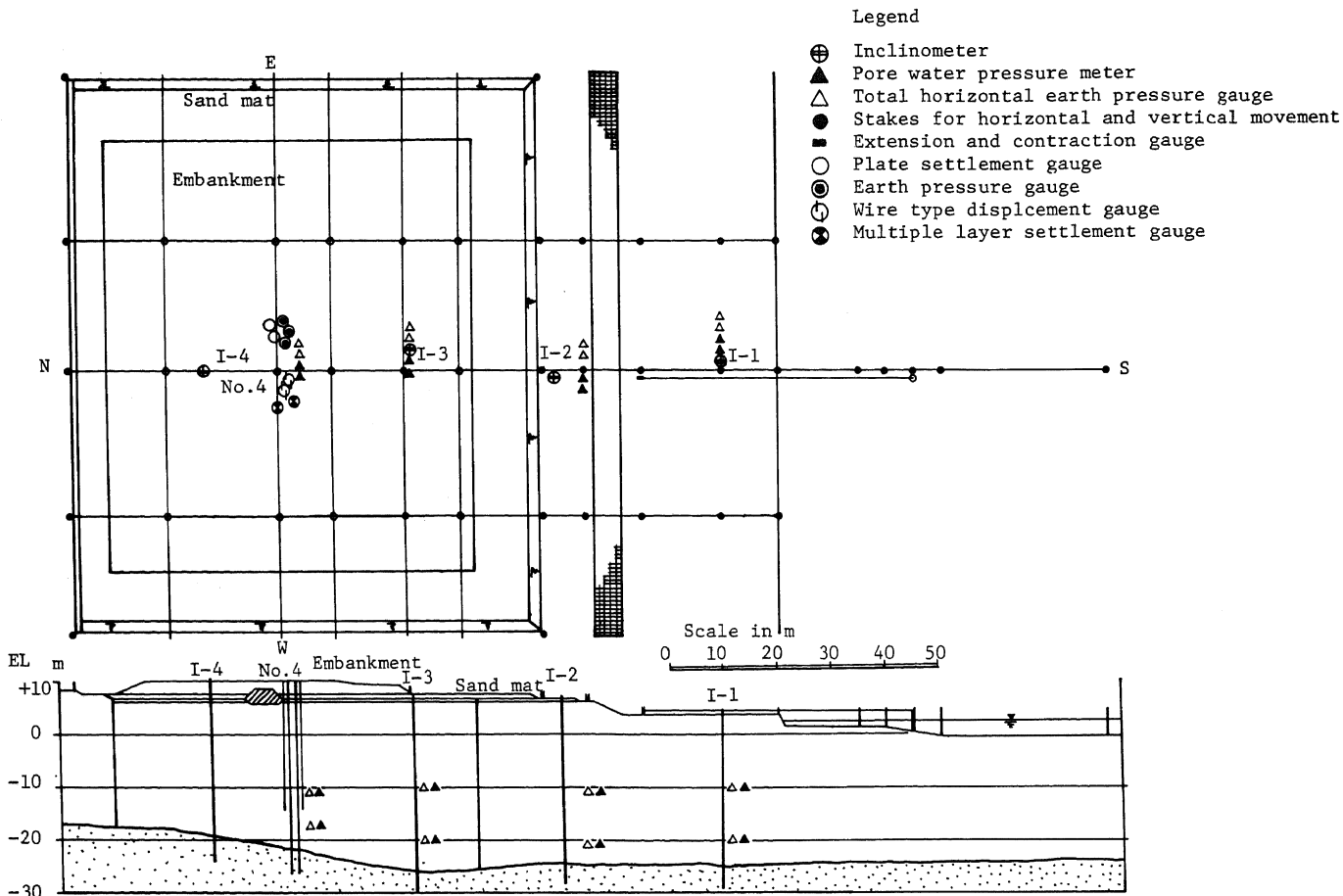


Fig. 3 Arrangement of Instruments

are indicated simply as 9. Two hundred and three piles were driven from July 9 to 20. Figure 6 gives the record of inclinometer measurement from July 9 to 20. Sliding along the old sliding surface at E.L. -23 m and shear deformation of soft layer between E.L. -10 m and -23 m mostly contributed to the displacement. Figure 7 shows the records of pore water pressure and horizontal total pressure, which arose as the pile driving operation and decreased suddenly after the pile driving operation stopped. Amount of fluctuation was about 10 kPa. Accumulated pressure is given in Table II.

TABLE II. Accumulated Pressure in kPa

E.L. m	July 9-20		July 9-Nov. 12	
	Total pressure	Pore water pressure	Total pressure	Pore water pressure
-10	10	10	16	22
-20	25	20	23	(39)

(39): Estimated

Judging from the records, the soil mass moved step by step due to the pressure which was generated by the pile driving operation. Assuming that the number of piles driven in a certain day (July 11th, for example) are n , and the distance between the center of piles and the point I-2 is D , then displacement of I-2

towards the south direction d can be computed from

$$d = \frac{kn \cos \beta}{D} \quad \text{----- (2)}$$

Putting the data from July 9 to 20 into eq.(2), k -value can be calculated, as given in Table III.

TABLE III.

Date	10	11	12	13	14	15	16	17	19	Mean
k	16	15	10	6	4	2	8	20	20	11

As the point I-2 moved by 120 m during the whole pile driving operation, k -value is calculated as 10. The horizontal displacement would be inversely proportional to the area ratio p (area of SCP to that of outer clay). As the area ratio p was 0.106 in this example, following empirical equation can be obtained,

$$d = \frac{6n \cos \beta}{D} \times \frac{p}{0.106} = \frac{57np \cos \beta}{D} \quad \text{----- (3)}$$

This sort of empirical equation should be obtained also for other case records.

STABILITY ANALYSIS BEFORE RECONSTRUCTION OF EMBANKMENT

Stability analysis before reconstruction of embankment was required, because the large movement was observed only by the SCP driving. For safety, 2.6 m high embankment was proposed

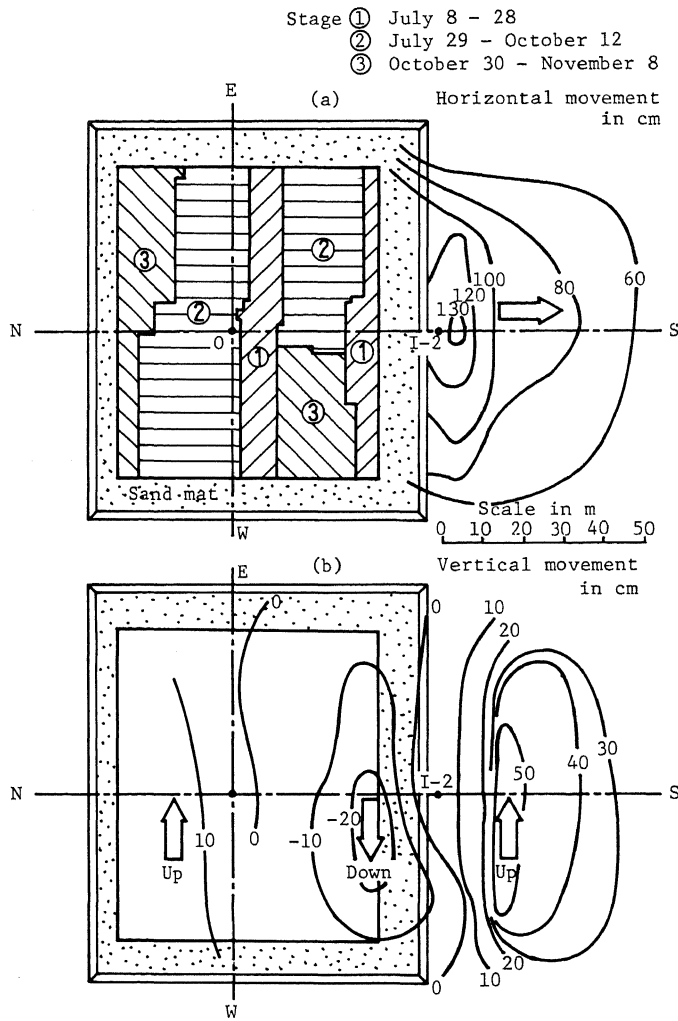


Fig.4 Movement of Ground Surface Caused by Sand Compaction Pile (SCP) Driving

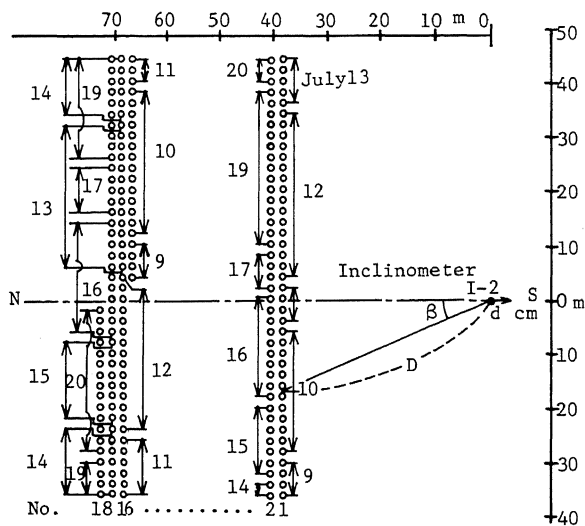


Fig.5 Sequence of Pile Driving

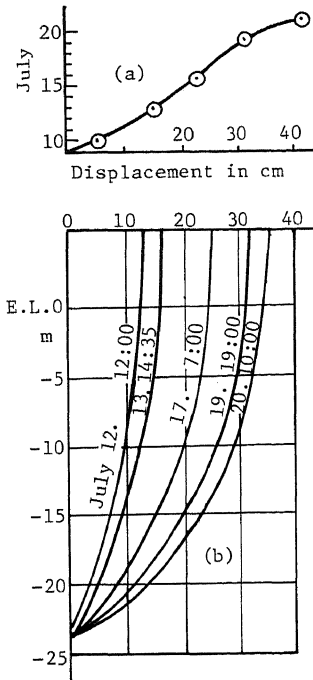


Fig. 6 Horizontal Displacement at I-2

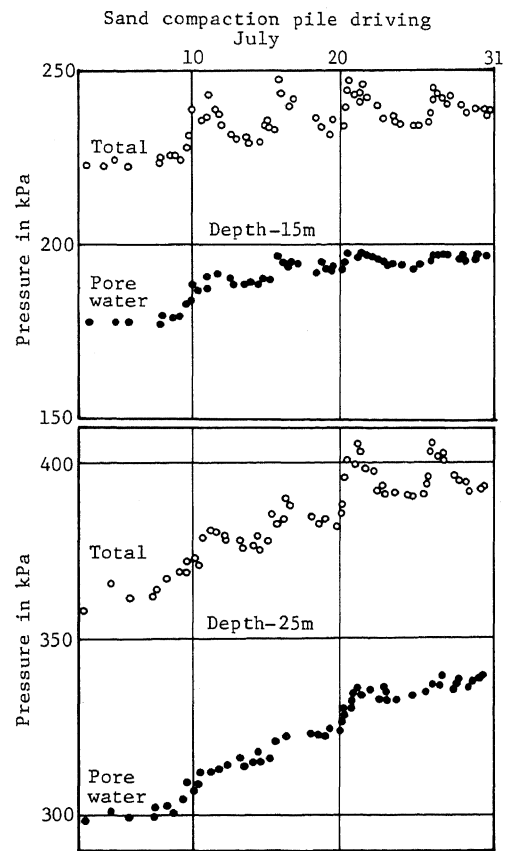


Fig. 7 Total and Pore Water Pressure Increase by Pile Driving at Point I-3

as the first stage of construction. Conventional stability analysis with a composite sliding surface gave a factor of safety nearly equal to unity. Moreover, this method seemed to be questionable since the total earth pressure on the assumed vertical wall which separated slices were unrealistic. Therefore, a more reliable stability analysis was contemplated utilizing the observed data and the soil testing results. Lack of observation data was felt at the beginning of the analysis. An engineering judgement was applied to some points. A model was constructed referring to Fig. 1. Figure 8 shows the model. Soil constants were back calculated with the previous slide. The following equation is obtained assuming the factor of safety is one.

$$F_s = \left[\left\{ (\gamma_e h_e B + \frac{\gamma_f}{2} BH) \sin \alpha - \frac{1}{2} \gamma_w \frac{H^2}{\cos \alpha} \right\} \tan \phi_c + \frac{H}{\cos \alpha} c \right] \div \left[(\gamma_e h_e B + \frac{\gamma_f}{2} BH) \cos \alpha - P_H \sin \alpha \right] \quad (4)$$

where,

- γ_e : unit weight of the embankment soil (kN/m^3),
 - h_e : height of the embankment (m),
 - B : width of the embankment (m),
 - γ_f : unit weight of the foundation soil (kN/m^3),
 - H : height of the assumed vertical wall in the foundation, ab (m),
 - P_H : total normal force acting against the wall, ab (kN/m),
 - α : angle bad (degrees),
 - ϕ_c : angle of internal friction of the foundation soil (degrees),
 - c : cohesion of the foundation soil (kPa).
- Putting the following figures into Eq. (4), combinations of c and ϕ_c are obtained as the calculated soil constants; $\gamma_e = 17 \text{ kN/m}^3$, $h_e = 4 \text{ m}$, $B = 20 \text{ m}$, $\gamma_f = 15 \text{ kN/m}^3$, $H = 30 \text{ m}$, $P_H = 6 \text{ MN/m}$.

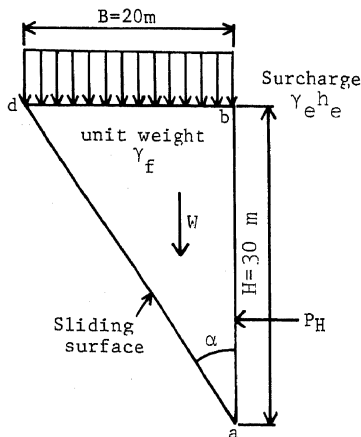


Fig. 8 Sketch of a Sliding Block under Embankment

The author adopted a combination of c and ϕ_c as 34.1 kPa and 10 degrees based on his experience of landslide investigation (Fig. 9). In the case of the embankment on the improved foundation with SCP, the method of analysis is very similar to the one proposed to the above analysis. The difference is to take into consideration the change in unit weight and the increase of strength due to the SCP. The excess pore water pressure at the surface ad is

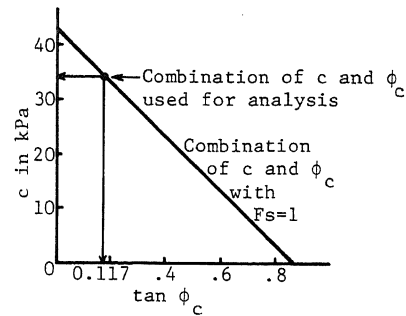


Fig. 9 Combination of $\tan \phi_c$ and c Which Satisfies Eq. (4)

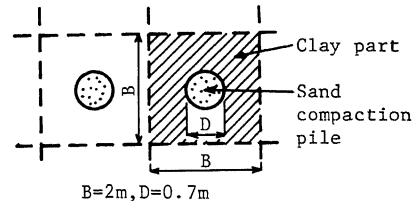


Fig. 10 Plan of Sand Compaction Pile (SCP)

neglected because the SCP were considered to function as a vertical drain. Assuming diameter and spacing of SCP D and B , respectively, the areas of a SCP and clay part outside the SCP are $\pi D^2/4$ and $B^2 - \pi D^2/4$, respectively. Area ratios with respect to the SCP and clay parts are $a_s = \frac{\pi D^2}{4} \div B^2$ and $a_c = (B^2 - \frac{\pi D^2}{4}) \div B^2$, respectively.

Assuming vertical stresses of SCP and clay part σ_s and σ_c , respectively, the rates of vertical total pressure beared by the SCP and the clay parts are calculated as

$m_s = \frac{na_s}{a_c + na_s}$ and $m_c = \frac{a_c}{a_c + na_s}$, respectively. The ratio $n = \sigma_s : \sigma_c$ is not known in this case, but this may be assumed to be 2 by engineering judgement. As $B = 2 \text{ m}$ and $D = 0.7 \text{ m}$, $m_s = 0.1752$ and $m_c = 0.8248$. Factor of safety is calculated as follows.

$$F_s = \left[\left\{ (\gamma_e h_e B + \frac{\gamma_{sc} BH}{2}) \sin \alpha + P_H \cos \alpha - \frac{1}{2} \gamma_w \frac{H^2}{\cos \alpha} (m_s \tan \phi_c + m_c \tan \phi_c) + \frac{H}{\cos \alpha} a_c c \right\} \right] \div \left[(\gamma_e h_e B + \frac{\gamma_{sc} BH}{2}) \cos \alpha - P_H \sin \alpha \right] \quad (5)$$

Unit weight of the improved foundation soil γ_{sc}

may easily be obtained as $\gamma_{sc} = 15.48 \text{ kN/m}^3$, assuming density of sands $\gamma_s = 20 \text{ kN/m}^3$.

Finally, the factor of safety, F_s is obtained with the embankment height $h_e = 4 \text{ m}$ and the unit weight $\gamma_e = 17 \text{ kN/m}^3$. It is very common to use the total stress method concerning $n = \sigma_s : \sigma_c$, but the total stress method might be more rigorous. Comparison of the two methods is discussed herein.

Vertical stress at a point of subsoil is expressed as $(p'+u)$, where p' and u are effective and neutral stress, respectively. The stresses at the clay part are written as

$$\frac{a_c}{a_c + na_s} (p'+u) \text{ based on the total stress method,}$$

$$\text{and } \frac{a_c}{a_c + na_s} p'+u \text{ by the effective stress method.}$$

For example, $p'=100$ kPa and $u=200$ kPa, together with the above a_s and a_c , give the stresses 247.4 kPa for the total stress method, and 282.5 kPa for the effective stress method. The difference is so large that it cannot be neglected.

If $n=3$ is taken into calculation instead of $n=2$, the factor of safety $F_s=1.11$ is obtained.

As it was proved that the 4 m high embankment can be constructed safely, go-sign was given to the construction of the 2.6 m high first stage embankment. The reconstruction work started with special care of installing many instruments for controlling.

BEHAVIOR OF TOTAL HORIZONTAL EARTH PRESSURE AND PORE WATER PRESSURE DURING RECONSTRUCTION OF EMBANKMENT

Figure 11 describes the observed records of the total horizontal earth pressure and the pore water pressure immediately before and after the sand compaction pile (SCP) driving and at the end of embankment construction. "t" stands for total horizontal earth pressure, and "u" pore water pressure. The total horizontal earth pressure at No. 2 (I-2), E.L. -10 m and -20 m increased 19 and 35 kN/m^2 , respectively,

during the SCP driving and decreased with time afterwards. The construction of the embankment stimulated the pore water increase, but the contribution was not enough to compensate the decreasing tendency following the pile driving. Such contribution would be the main reason why the displacement during the embankment construction was so small. No pressure increase was observed at No. 1 (I-1). Those pressure gauges installed middle and the foot of the embankment, namely No. 4 and 3 (I-3), were fluctuating in their observed values. Increases of the pressures during the SCP driving at these points might have been larger than those at the other two points. Therefore, such records would have been obtained.

GROUND MOVEMENT DURING RECONSTRUCTION OF EMBANKMENT

As stated above, movement of foundation was unexpectedly small. Figure 12 shows the movement of the ground surface. The ground surface near the point I-2 moved towards the embankment, namely to the north, and settled down at the same time. The inclinometer records showed that movement near the ground surface directed to north and soils at deeper position moved to south. Maximum displacement was observed at E.L. -10 m. Sign of sliding along the old sliding surface was observed. After-effect of the SCP driving and drag-effect of the embankment were acting reversely.

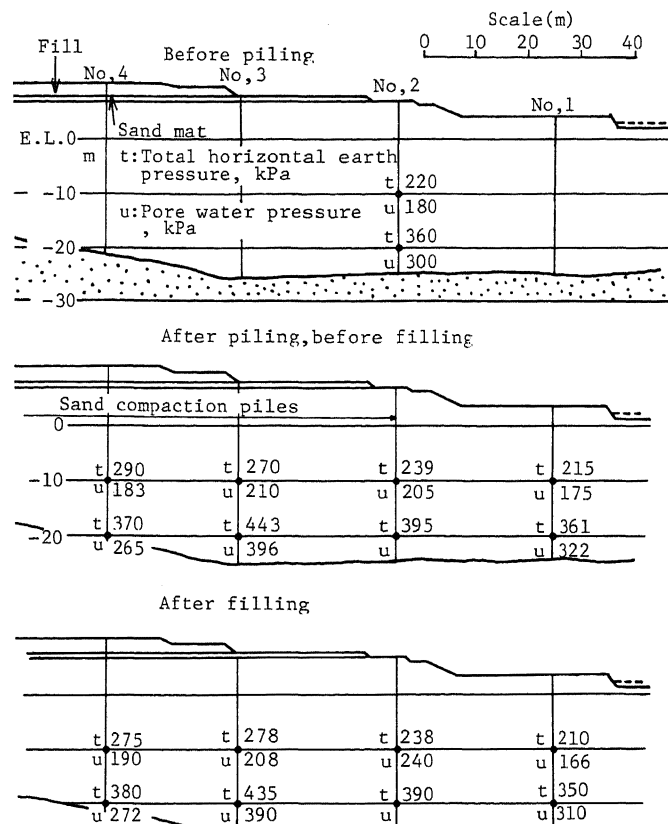


Fig. 11 Total Horizontal Pressure and Pore Water Pressure Measured

Therefore, movement of the ground became more complicated.

Multiple layer settlement gauge was installed in a borehole to obtain settlements at eleven points in the borehole. The spacing of the measuring points was 3 m. One of the gauges was installed at the middle of the SCP, and the others outside the SCP. Amount of contraction was calculated based on the observed records and illustrated in Table IV. Especially large contraction was observed at the soft clay layer between E.L. -12.5 m and -17.5 m. Rate of contraction was approximately the same with inside and outside of the sand compaction pile.

SUSTAINING RATIO OF SAND COMPACTION PILE (SCP)

"Sustaining ratio of SCP", n , is defined as the ratio between vertical stress of the sand compaction pile and that of the clay part outside the SCP. This ratio is regarded to be constant through the SCP in the stability analysis. In this case, n was assumed to be equal to 2. Importance of n -value may be clear from the following calculation. Effect of SCP used for improving soft clay foundation may be exhibited by reduction of load sustained by soft clay layer. Degree of effectiveness may be expressed in terms of coefficient of "load reduction factor", r_d , which is defined as the ratio between vertical pressure increment due

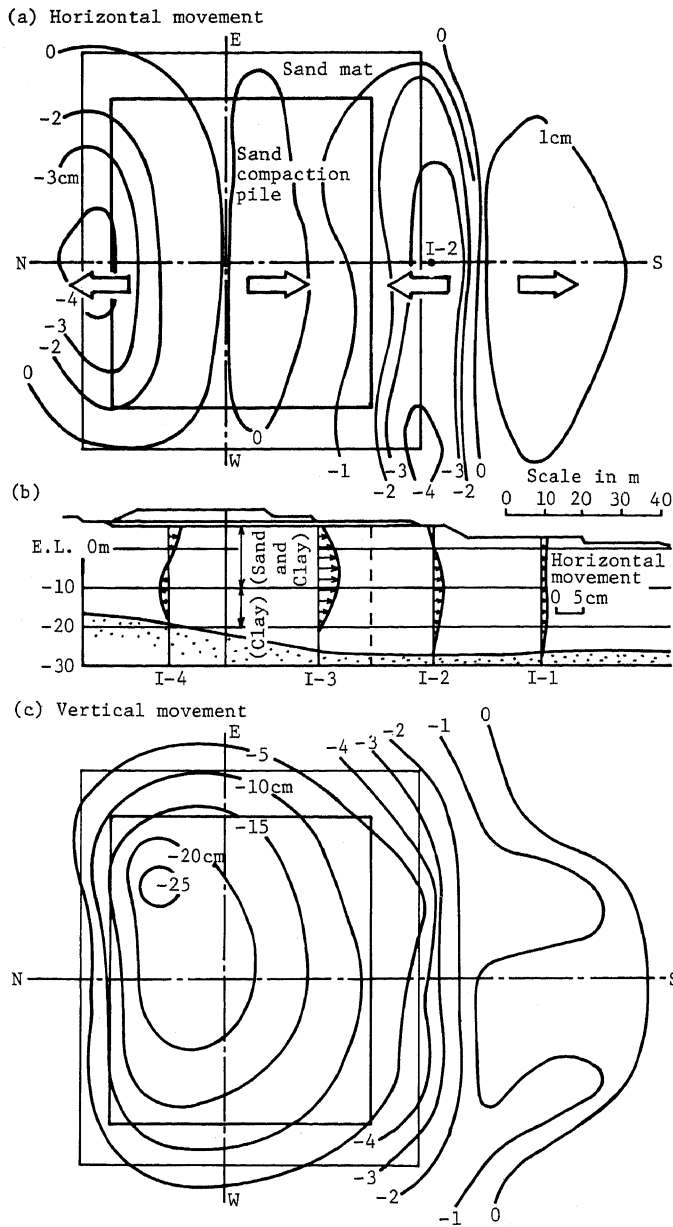


Fig. 12 Movement of Ground during Filling Operation

to a surcharge with SCP and that without SCP.

$$r_d = 1 + \frac{\pi(n-1)}{4} \left(\frac{D}{B}\right)^2 + 1 \quad \text{----- (6)}$$

Assuming $D=0.7$ m; $B=2$ m and 3 m; $n=1, 2, 3, 4$ and 5; the results of calculation are given in Fig. 14. If $n=2$ and $B=2$ m, then $r_d=0.912$. If we aim at the load reduction factor $r_d=0.912$,

spacing of the SCP differs from 2 m to 3 m, according to the evaluation of the n -value from 2 to 3. Number of piles per unit area is in reverse proportion to square of the pile spacing. Cost of 2 m spacing SCP is 2.25 times more expensive than that of 3 m spacing SCP. This simple calculation would be enough to show importance of the n -value.

TABLE IV. Contraction of SCP and Clay Layer

E.L. m	SCP	Clay layer
+5.5 to +2.5	0.855	1.655
+2.5 to -0.5	0.690	0.515
-0.5 to -3.5	1.310	1.415
-3.5 to -6.5	1.945	1.465
-6.5 to -9.5	1.645	1.915
-9.5 to -12.5	1.670	2.965
-12.5 to -15.5	6.730	5.435
-15.5 to -18.5	4.070	4.260
-18.5 to -21.5	1.680	1.740
-21.5 to -24.5	1.240	0.595

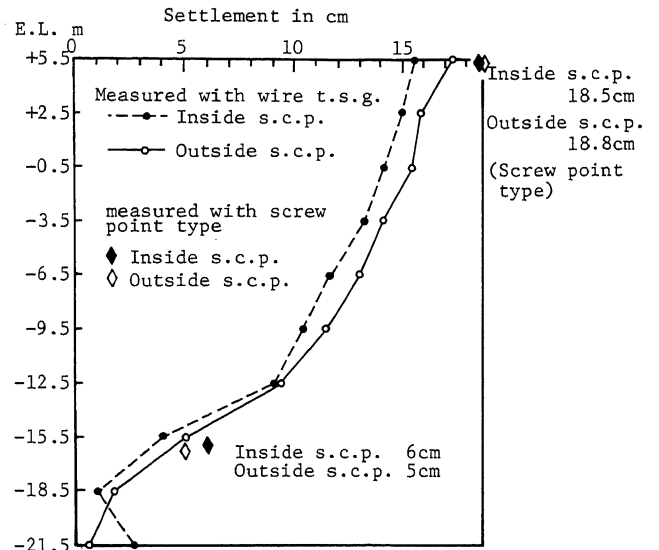


Fig. 13 Settlement of Points in Soft Ground with the Multiple Layer Settlement Gauge

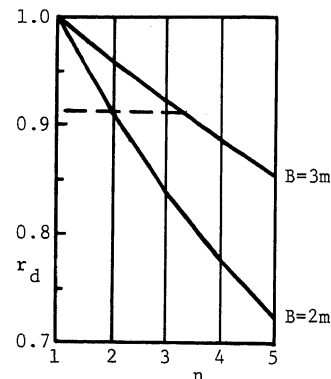


Fig. 14 Relationship between n , r_d and B

Methods of estimating the n -value have been proposed by many engineers in Japan. One of them is the method proposed by Prof. K. Yamagata, et al. last year. Their idea was that an SCP was regarded as a precast concrete pile subjected to negative skin friction. Figure 15 gives the proposed model.

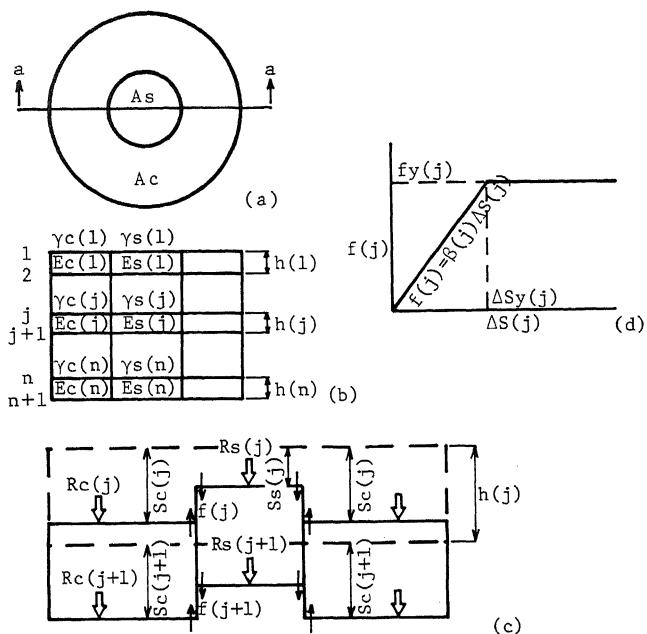


Fig. 15 Model of SCP (K. Yamagata)

Figure 15 (a) is a plan of the SCP and the clay part outside the SCP. The a-a section is given in (b). The sand and clay layers are numbered (1), (2), ---- from the top to the bottom. γ and E are unit weights and moduli of deformation, respectively. The suffixes, c and s represent clay and sand, respectively. The element of the SCP is magnified as shown in (c). Wall friction is assumed to be produced by relative movement of sand and clay. A model of friction is given in (d). The stresses acting on the j plane are,

$$\bar{\sigma}_s(j) = \frac{1}{A_s} \left\{ R_s(1) + \frac{1}{2} \psi F(j) \right\} + \sum_{i=1}^{j-1} h(i) \gamma_s(i) \quad \text{---- (7)}$$

$$\bar{\sigma}_c(j) = \frac{1}{A_s} \left\{ R_c(1) - \frac{1}{2} \psi F(j) \right\} + \sum_{i=1}^{j-1} h(i) \gamma_c(i) \quad \text{---- (8)}$$

$$n(j) = \frac{\sigma_s(j)}{\bar{\sigma}_c(j)} \quad \text{----- (9)}$$

where,

$$F(j) = f(1) \cdot h(1) + f(j) \cdot h(j) + 2 f(2) \cdot h(2) + f(3) \cdot h(3) + \dots + f(j-1) \cdot h(j-1)$$

ψ : perimeter of SCP

Standard penetration test was performed at the center of the SCP near the multiple layer settlement gauge. The results were,

E.L. m	N-value
+6 to +1.5	10
+1.5 to -9.0	20 to 35 mean 27
-9.0 to -17.0	25 to 35, mean 30

Soil constants are assumed to be those shown in Table V. The last column is the results of calculation.

Assuming the settlements of the plates which measured settlement of the SCP and nearby ground surface gave correct values. Every layer

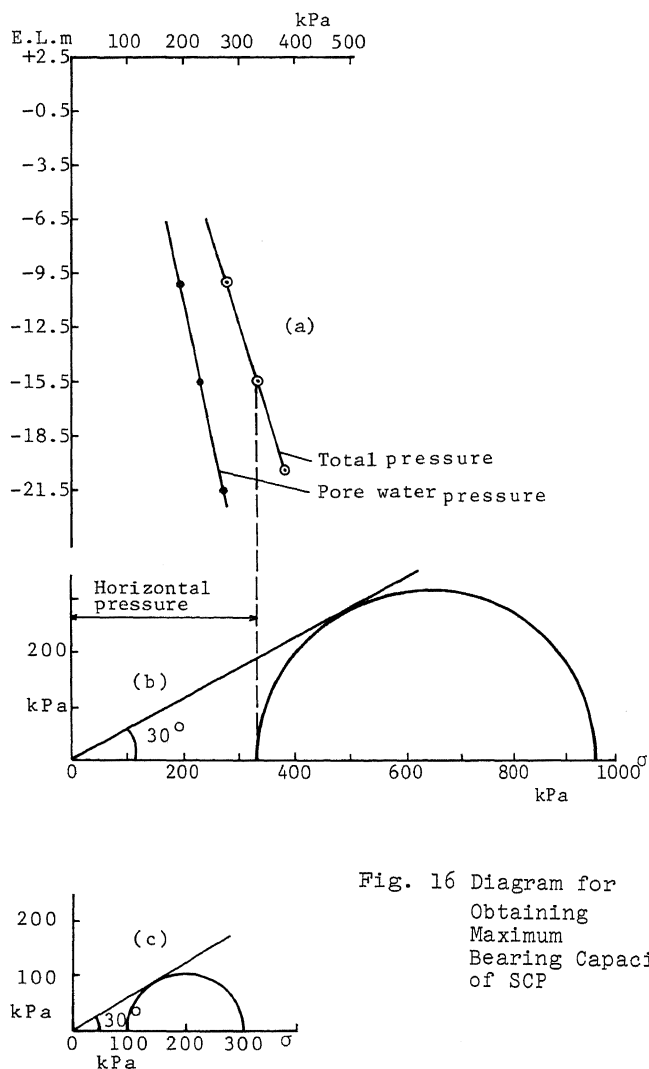


Fig. 16 Diagram for Obtaining Maximum Bearing Capacity of SCP

TABLE V. Soil Constants and n-Value

E.L. (m)	E_s (MPa)	E_c (MPa)	f_y (kPa)	S (m)	n
+5.5 to -0.5	7.0	5.0	65	0.01	1.4
-5.0 to -9.5	10.0	3.0	50	0.01	3.4
-9.5 to -21.5	15.0	1.0	40	0.01	15.0

of sand and clay settled in horizontal plane. Then, the n -value is proportional to $E_s : E_c$, where E_s and E_c denote the coefficients of deformation for sand and clay, respectively. Plate bearing tests were performed to get the coefficients of deformation at the base of the embankment. The k -values on the sand and clay were 35 MN/m^3 and 13.5 MN/m^3 , and the coefficients of deformation 135 MN/m^2 and 50.3 MN/m^2 , respectively. Then $n=2.6$ was obtained. Two earth pressure gauges were installed at the top of the SCP and outside the nearby SCP. n -value was about 2 at the beginning of measurement, then decreased with time. The earth pressure gauges showed very small earth

pressures. Earth pressure gauges cannot be used at deeper positions. Therefore, indirect method had to be used to find out the n -value. n -value at E.L. -9.5 to -21.5 m in Table V seems to be too large. Therefore, further discussion was made. It is very common to apply the total stress method in discussion of n -value. Sometimes it seems to be better to adopt the effective stress method. The total horizontal pressures at two depths are plotted in Fig. 16 (a). The total horizontal earth pressure and pore water pressure at E.L. -15.5 m were obtained with interpolation. The vertical stresses at the point can be calculated. Figure 15 (b) and (c) represent the cases of the total and effective states, respectively. Mohr's rupture lines are drawn in those figures, assuming the angle of internal friction $\phi=30^\circ$. First, the horizontal earth pressures are plotted on the horizontal axes of those figures. The maximum vertical stresses are obtained as 950 and 310 kN/m^2 from those figures. Assuming the unit weight of the embankment and foundation with SCP 17 and 15.48 kN/m^3 , respectively, the total vertical stresses upon the clay can be obtained. In case the vertical stress of the SCP reaches the maximum value, the vertical stress of the clay part may increase in response to it. The calculated values are given in Table VI.

TABLE VI n -Value at E.L. -15.5 m

	Sand		Clay		n
	Stress Force (kPa)	Stress Force ($\text{kN}/4\text{m}^2$)	Stress Force (kPa)	Stress Force ($\text{kN}/4\text{m}^2$)	
Total(b)	950	365.6	256	925.7	3.7
Effective(c)	310	119.3	70	371.4	4.4

SCP applied to soft soils has been evaluated only from view point of n -value, but increase of horizontal pressure was found to be very effective to increase shear strength of soft soils in this case. The unconfined compression tests with samples taken from the site showed very high strength (Fig. 17).

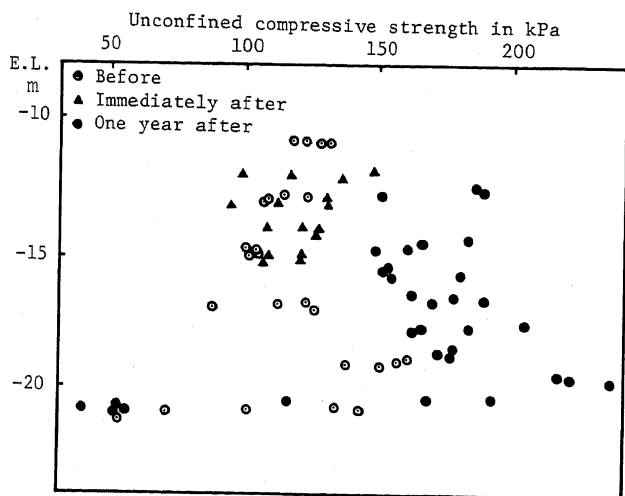


Fig. 17 Unconfined Compressive Strength of Clays, before, Immediately after and One Year after SCP Driving

CONCLUSIONS

A deep seated failure with a composite sliding surface took place during construction of low embankment. It was explained with unbalance of earth pressure on two assumed vertical walls. Sand compaction piles (SCP) were driven into the slid soft ground as the soil improvement work. Large horizontal and vertical movement was observed. A sliding along the previous sliding surface was recognized. Therefore, another sliding was feared, and a stability analysis based on the observed data and soil testing results was performed. Careful embankment construction work was carried out with measuring total horizontal pressure, pore water pressure and displacement. Complicated movement was observed because of non uniform soil layer, previous slide and after-effect of sand compaction pile driving. Movement of the ground was very small during the filling operation, and the first stage of construction was completed successfully.

Stress ratio of sand and outer clay was important for the design of the sand compaction pile. The multiple layer settlement gauges were installed both inside and outside of the sand compaction pile, and difference of contraction of layers were measured. It was found that further research work should be encouraged.

Sand compaction piles press outer clay layer horizontally and remarkably increases strength of soft clay.

ACKNOWLEDGEMENT

The original data were provided by the Fudo Corporation and OYO Corporation. The author expresses his deepest appreciation to those engineers who engaged in this construction work.

REFERENCES

- Ad hoc Committee of Case Studies of Coastal Reclamation (1981), "Geotechnical Aspects of Coastal Reclamation Projects in Japan", Proc 9th International Conference on Soil Mechanics and Foundation Engineering, Case History Volume, pp.599-664, Tokyo, Japan.
- Ad hoc Committee of Case Studies of Soft Ground (1981), "Embankment Works on Soft Grounds", Proc., 9th International Conference on Soil Mech. and Foundation Engineering, Case History Volume, pp. 665-724, Tokyo, Japan
- Yamagata, K., K. Fukumoto, (1982), "Stress Ratio of Sand and Outer Clay in Composite Ground", Proc., 17th Japanese Symposium on Soil Mechanics and Foundation Engineering, Vol. 2.2, pp. 2417-2420, Naha City, Japan. (in Japanese)